Tortuosity of Pulmonary Vessels Correlates with Pulmonary Hypertension

Michael Helmberger[13]
m.helmberger@student.tugraz.at
Martin Urschler[12]
martin.urschler@cfi.lbg.ac.at
Zoltán Bálint[3]
zoltan.balint@lvr.lbg.ac.at
Michael Pienn[3]
michael.pienn@lvr.lbg.ac.at
Andrea Olschewski[3]
andrea.olschewski@lvr.lbg.ac.at
Horst Bischof[1]
bischof@icg.tu-graz.ac.at

[1] Inst. f. Computer Graphics & Vision
Graz University of Technology
Graz, Austria

[2] Ludwig Boltzmann Institute for
Clinical-Forensic Imaging
Graz, Austria

[3] Ludwig Boltzmann Institute for Lung
Vascular Research
Graz, Austria

Abstract

Pulmonary hypertension (PH) is a chronic disorder of the pulmonary circulation, marked by an elevated vascular resistance and pressure. Our objective is to find an automatic, non-invasive method for estimating the pulmonary pressure based on the analysis of lung vessels from contrast enhanced CT images. We present a pulmonary vessel extraction algorithm which is fast, fully automatic and robust. It uses an airway tree segmentation and a left and right lung labeled volume to restrict the response of an offset medialness vessel enhancement filter. On a data set of 24 patients, we show that quantitative indices derived from the vascular tree are applicable to distinguish patients with and without PH.

1 Introduction

Pulmonary hypertension is a type of disease presenting high blood pressure in the lung vessels. PH is defined as a mean pulmonary arterial pressure (mPAP) ≥ 25 mmHg, and the gold standard for determining it is invasive right-heart catheterisation (RHC) [9]. In severe cases PH results in a markedly decreased exercise tolerance and heart failure.

A non-invasive alternative to RHC would be beneficial for diagnosis of PH. We investigate the hypothesis, that a quantitative index of lung vascular tree structure, acquired by a contrast enhanced CT, is correlated with PH. For vessel detection, we propose an algorithm that uses a combination of lung- and airway segmentation, together with a sophisticated vessel enhancement filter to obtain a proper segmentation of the left and right pulmonary vessel trees separately, even in patients showing severe pathologies. The algorithm is fully automatic, computationally efficient and able to handle large datasets. Analysis of the vessel tree

is based on two readouts, the fractal dimension (FD) and tortuosity, which are computed from the obtained vascular tree and compared to the patient's clinical data derived from RHC.

1.1 Related Work

A large number of 3D vessel segmentation algorithms for investigating, e.g. pulmonary vessel trees, coronary arteries, or brain vessels have been presented in the literature. Typical algorithms are based on vessel enhancement filters, which analyse the eigenvalues and -vectors of the Hessian matrix [4]. A recent, comprehensive overview of different enhancement and segmentation techniques can be found in [5].

Previous works showed a correlation of the pulmonary vascular tree complexity with PH. In [6] FD is reported to correlate with pulmonary vascular resistance in children suffering from PH. In [3] it was shown, that the FD of the pulmonary arteries in PH patients is highly correlated with mPAP. However, these two studies use maximum intensity projections (MIP) of the vessel trees to compute the FD, whereas we calculate our quantitative readouts in 3D. We are not aware of any work that correlates vessel tortuosity with PH.

2 Method

At the core of our method is a multi-scale vessel enhancement (VE) filter based on the Hessian matrix. It is a modified version of [8], and uses the eigenvalues of the Hessian matrix to detect candidate voxels inside the vessels, and an offset-medialness boundary measure perpendicular to the estimated vessel direction to compute the vessel probability [4]. The medialness is limited to the right and left lung, which is derived from an intensity-based lung segmentation. After non-maximum suppression of the medialness, the centerlines are detected and connected using a shortest path approach. Figure 1 shows the flowchart of our automatic vessel detection.

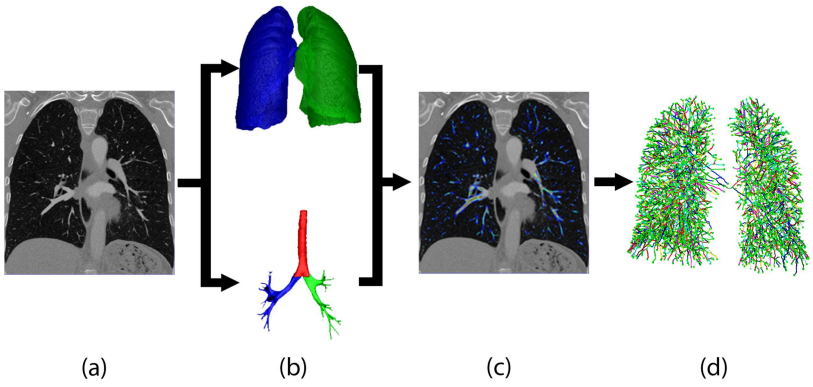

Figure 1: Vessel extraction flowchart. (a) input CT-image, (b) lung- and airway segmentation, (c) medialness restricted to the lung (blue: high vessel probability), (d) vascular tree

2.1 Lung and airway segmentation

A prerequisite for our vascular tree extraction is a segmentation of left and right lungs, respectively, to restrict the reconnection of the vessel centerlines. We use a coarse airway segmentation consisting of an iterative region growing procedure starting at the trachea, and

a labeling into left and right airway tree (separated at the carina). This labeled airway tree is taken to divide a threshold based lung segmentation into left and right lung, respectively, followed by morphological closing to refine the lung segmentations. The airways guarantee proper separation even in difficult cases as it is presented on Figure 2.

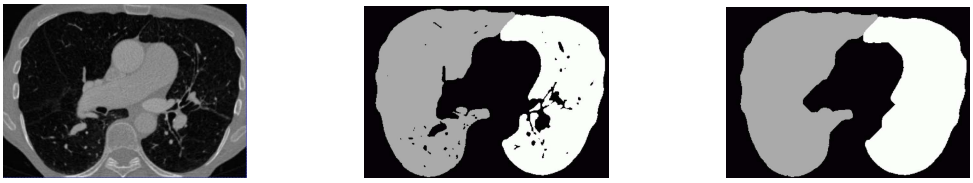

(a) (b) (c)

Figure 2: (a) example CT image, (b) coarse lung segmentation after separation, (c) refined lung segmentation, separate left (gray) and right (white) lung

2.2 Vessel enhancement

We enhance vessel like structures using a modified version of the vessel enhancement filter proposed by Pock et al. [8]. It uses the eigenvectors and values of the Hessian matrix, combined with an offset medialness response to estimate a vessel probability. The airway- and lung segmentations from Section 2.1 are used to restrict the vessel enhancement output to the region of interest, i.e. the lungs without the airways. To detect a wide range of different vessel radii, the filter is embedded within a multi-scale framework.

To get the vessel enhancement filter response, we calculate the eigenvalues $|e_1| \geq |e_2| \geq |e_3|$ and the associated eigenvectors $\mathbf{v_1}$, $\mathbf{v_2}$ and $\mathbf{v_3}$ of the Hessian matrix $\mathscr{H}^\sigma(\mathbf{x})$ at each scale σ. To sort out bright tubular structures on dark background we check that $e_1 < 0$ and $e_2 < 0$ holds. In points that fulfill this condition, the smallest eigenvector $\mathbf{v_3}$ gives an estimation for the vessel direction. Perpendicular to the vessel direction, in the cross section plane of the tube given by the eigenvectors $\mathbf{v_1}$ and $\mathbf{v_2}$, we evaluate boundary information along circles of different radii r. We define the boundary gradient $\mathbf{B}(\mathbf{x}) = \sigma \nabla I^\sigma(\mathbf{x})$, with $I^\sigma(\mathbf{x})$ being the CT image convolved with a Gaussian kernel with variance σ. An initial response is given by the median of the $N = \lfloor 2\pi r + 1 \rfloor$ boundary contributions $b_i = |\mathbf{B}(\mathbf{x} + r\mathbf{v}_{\alpha_i})\mathbf{v}_{\alpha_i}|$, which we denote as R_0^+. A problem of $R_0^+(x,r)$ is that it also produces responses at isolated edges. To avoid this, a measure of symmetry is introduced:

$$S(\mathbf{x},r) = 1 - \frac{s(\mathbf{x},r)}{\bar{b}}$$

where $s(\mathbf{x},r)$ is the median absolute deviation of the boundary samples and $\bar{b}$ the median. The final boundary response is computed as:

$$R^+(\mathbf{x},r) = R_0^+(\mathbf{x},r)S(\mathbf{x},r)^{\frac{3}{2}}$$

To suppress responses at the border of vessels, the gradient magnitude at the center of the vessel is combined with the offset medialness from above:

$$R(\mathbf{x}) = \max\{R^+(\mathbf{x},r) - \sigma|\nabla I^\sigma(\mathbf{x})|, 0\}$$

The final vesselness response is the maximum response from all different scales and radii.

2.3 Centerline extraction

In a non-maximum suppression step [1], at each position $\mathbf{x}$ with a medialness $R(\mathbf{x}) > th_{min}$, we sample 8 points on a circle in the plane perpendicular to the estimated vessel direction. If the medialness response at $\mathbf{x}$ is smaller than on any of those 8 sampled points, it is set to zero. This results in a large number of vessel centerline fragments. The centerlines are not connected, because at branching points, where the tubularity assumption fails, we get a low medialness response. Next, small centerline fragments (less than 5 N_{26}-connected voxels) are removed, and all maxima lying on the airway border are cleared. To reconnect the centerline fragments, we apply a Dijkstra-like shortest path algorithm. At each lung separately, we connect all centerline candidate points to the center of the image. As a cost function we combine the medialness with the gradient magnitudes of the CT image. The separate processing of right and left lung ensures avoiding wrong connections through the mediastinum. The merged trees from right and left lung form the final vessel tree (see Fig. 3).

(a) (b)

Figure 3: Representative results showing a patient with (a) and one without PH (b). No visual differences in the structure of the vascular trees are apparent.

3 Analysis of the pulmonary vascular tree

Our clinical application is the detection of PH, a chronic disorder of the pulmonary circulation, marked by elevated vascular resistance and mean pulmonary arterial pressure (mPAP), respectively. Our hypothesis is, that the structure of the pulmonary vascular tree shows quantifiable differences between healthy patients and patients diagnosed with PH. For analysis we compute two measures: the fractal dimension (FD) and the distance metric (DM). Our patient cohort from the clinical study consisted of 24 patients, who underwent contrast enhanced CT.

3.1 Fractal Dimension

The fractal dimension of the vessel centerlines was calculated by applying a 3D extension of the well-validated box counting method [3]. Box counting consists of dividing the vessel centerline image into a grid of equal boxes with size δ, and counting the number of boxes containing part of the vessel centerlines. This process is repeated for different box sizes (from one pixel up to 100 pixel side length). The fractal dimension is equivalent to the slope of a line fitted on a double logarithmic plot of the number of boxes against the box size δ.

3.2 Distance Metric

Another quantifiable property of the vessels is their tortuosity, which is a readout of twistedness [2]. The most common metric of vascular tortuosity is the distance metric, which

provides a ratio of the actual vessel length to the linear distance between its endpoints. We split the vascular tree into vessel segments, where a segment is defined as the path between two branching points or between a branching- and an end point of a vessel. The 3D length of the vessel segment d_l divided by the Euclidean distance between its endpoints d_e (Figure 4) results in a dimensionless number. The distance metric is calculated for all pulmonary vessel segments and the mean is taken for quantitative analysis.

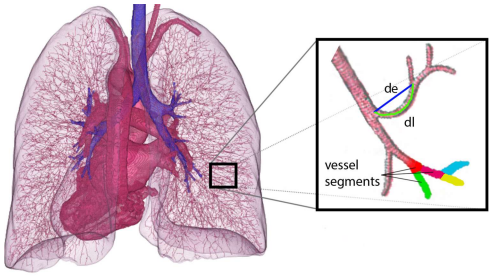

Figure 4: 3D rendering of vessel centerlines with the bronchi (blue) and the heart with main pulmonary vessels (red). Inset shows the computation of the distance metric. The length of the vessel segment is divided by the Euclidean distance between the two endpoints, $DM = \frac{d_l}{d_e}$.

4 Results

We found a correlation between mPAP and the DM of r = 0.69 (Pearson, p = 0.0002) (Figure 5a). As expected, there was a correlation of DM with the pulmonary vascular resistance (PVR; Pearson r = 0.66, p = 0.0004, Figure 5b) as this parameter correlates with mPAP. The ROC curve shows a discriminative power of this parameter with an AUC = 0.87 (Figure 5c). There was a significant difference between the DM of patients with PH and without PH (Table 1). The mean value of the FD in our patient cohort was 2.35, which is in good agreement with previously reported values from similar studies [7]. There was no difference between the 3D FD of patients with and without PH (Table 1). Moreover, no correlation of 3D FD with mPAP or PVR could be observed.

Readout	All patients (n=24)	No PH (n=6)		PH (n=18)
Distance metric	1.224 ± 0.019 (1.199 – 1.273)	1.208 ± 0.009 (1.199 – 1.223)	*	1.230 ± 0.019 (1.202 – 1.273)
Fractal dimension	2.35 ± 0.06 (2.21 – 2.44)	2.37 ± 0.08 (2.21 – 2.43)	ns	2.34 ± 0.05 (2.27 – 2.44)

Table 1: Values of distance metric and fractal dimension. Data are presented as mean±SD (range). The significance was tested with t-test (* $p < 0.05$, ns = not significant).

5 Conclusion

We have presented a fully automatic approach for vascular tree extraction and analysis from CT images based on a multi-scale vessel enhancement filter. Due to a parallel GPU implementation, it processes high-resolution CT data in around 10 minutes, thus enabling the potential use in daily clinical routine. On 24 patients from a clinical PH study, we showed

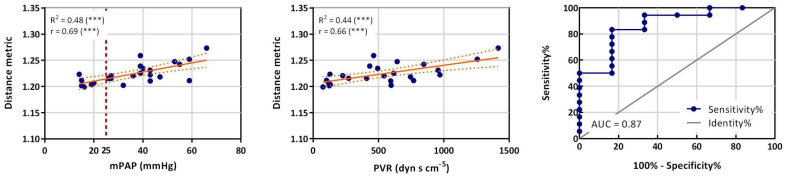

Figure 5: Correlation of distance metric (DM) with (a) mean pulmonary arterial pressure (mPAP), and (b) pulmonary vascular resistance (PVR; R = linear correlation coefficient, r = Pearson correlation coefficient, *** p<0.001). (c) Receiver-operator curve for DM determining mPAP $\geq$ 25 mmHg (AUC: area under the curve).

that there is no correlation between PH and FD. The correlations reported in [3] are likely due to their patient cohort consisting of children where the lung is still under development, or due to the MIP's used in the study [6]. In adult patients we have found that tortuosity instead of FD is correlated with pulmonary hypertension, showing the feasibility of non-invasive detection of PH with our vessel extraction and analysis algorithm in contrast enhanced CT.

References

[1] C. Bauer, T. Pock, E. Sorantin, H. Bischof, and R. Beichel. Segmentation of interwoven 3d tubular tree structures utilizing shape priors and graph cuts. *Medical Image Analysis*, 14(2):172–184, 2010.

[2] E. Bullitt, G. Gerig, S. M. Pizer, W. Lin, and S. R. Aylward. Measuring tortuosity of the intracerebral vasculature from mra images. *IEEE Transactions on Medical Imaging*, 22:1163–1171, 2003.

[3] S. Haitao, L. Ning, G. Lijun, G. Fei, and L. Cheng. Fractal dimension analysis of mdct images for quantifying the morphological changes of the pulmonary artery tree in patients with pulmonary hypertension. *Korean J Radiol*, 12:289–96, 2011.

[4] K. Krissian, G. Malandain, N. Ayache, R. Vaillant, and Y. Trousset. Model-based detection of tubular structures in 3d images. *Computer Vision and Image Understanding*, 80(2):130–171, 2000.

[5] D. Lesage, E. Angelini, I. Bloch, and G. Funka-Lea. A review of 3d vessel lumen segmentation techniques: Models, features and extraction schemes. *Medical Image Analysis*, 13(6):819–845, 2009.

[6] S. Moledina, A. de Bruyn, S. Schievano et al. Fractal branching quantifies vascular changes and predicts survival in pulmonary hypertension: a proof of principle study. *Heart*, 97(15):1245–1249, 2011.

[7] B. Mueller, S. Lang, F. Beckmann et al. Comparing the micro-vascular structure of cancerous and healthy tissues. In *Proc. SPIE 8506, Developments in X-Ray Tomography VII*, 2012.

[8] T. Pock, R. Beichel, and H. Bischof. A novel robust tube detection filter for 3d centerline extraction. In *Image Analysis*, volume 3540 of *Lecture Notes in Computer Science*, pages 481–490. Springer Berlin Heidelberg, 2005.

[9] G. Simonneau, I. Robbins, M. Beghetti et al. Updated clinical classification of pulmonary hypertension. *Journal of the American College of Cardiology*, 54(1, Supplement):43–54, 2009.